Probing the Wave Function Delocalization in CdSe/CdS Dot-in-Rod Nanocrystals by Time- and Temperature-Resolved Spectroscopy

Gabriele Rainò,[†,*] Thilo Stöferle,[†] Iwan Moreels,[†,‡] Raquel Gomes,[‡] John S. Kamal,[‡] Zeger Hens,[‡,*] and Rainer F. Mahrt[†,*]

[†]IBM Research Zurich, Säumerstrasse 4, 8803 Rüschlikon, Switzerland, and [‡]Physics and Chemistry of Nanostructures, Ghent University, Krijgslaan 281-S3, B-9000 Gent, Belgium

ABSTRACT Colloidal semiconductor quantum structures allow controlling the strong confinement of charge carriers through material composition and geometry. Besides being a unique platform to study fundamental effects, these materials attracted considerable interest due to their potential in opto-electronic and quantum communication applications. Heteronanostructures like CdSe/CdS offer new prospects to tailor their optical properties as they take advantage of a small conduction band offset allowing tunability of the electron delocalization from type-I toward quasi-type-II. Here, we report on a detailed study of the exciton recombination dynamics in CdSe/CdS heterorods. We observed a clear size-dependent radiative lifetime, which can be linked to the different degree of electron wave function (de)localization. Moreover, by increasing the temperature from 70 to 300 K, we observed a considerable increase of the radiative lifetime, clearly demonstrating a reduction of the conduction band offset at higher temperatures. Understanding and controlling electron delocalization in such heterostructures will be pivotal for realizing efficient and low-cost photonic devices.

KEYWORDS: colloidal nanocrystals · band alignment · exciton dynamics

Colloidal semiconductor nanocrystals have great potential for applications in opto-electronic devices such as LEDs, lasers, and photovoltaic cells[1−3] due to their widely tunable electro-optic properties. Precise control of the charge carrier localization is prerequisite to a successful implementation of these materials in practical devices. This can be achieved by the growth of core/shell heterostructures that enable the engineering of the band alignment and the spatial distribution of the electron and hole wave functions by combining semiconductors with different energy gaps. In particular, with the so-called type-I band alignment, the core of the nanocrystal is surrounded by a shell having a wider band gap such that the minimum of the conduction band (CB) and the maximum of the valence band (VB) are both in the core. As a result, excitons are confined to the core, typically leading to high and stable photoluminescence quantum yields. On the other hand, in type-II heterostructures, the band extrema are located in different materials. This leads to spatially separated excitons, a configuration finding its natural implementation in photovoltaic devices, switches, and lasers.[4] Recently, a new class of heterostructures attracted attention. Here, a spherical CdSe core is covered by a rod-shaped CdS shell (Figure 1a), resulting in a configuration intermediate between type-I and type-II. Such heteronanostructures can be produced with narrow size distributions and a small number of defects, and thus can exhibit an extraordinarily high quantum yield (as high as 75%).[5−7] Attractive new opto-electronic properties arise from the mixed dimensionality in which the zero-dimensional core structure is surrounded by the one-dimensional rod-shaped shell. Indeed, a wealth of interesting physical properties have already been observed, such as an exceptional size-dependent quantum-confined Stark effect,[4,8] suppression of the single-dot photoluminescence blinking,[9] and suppression of the Auger recombination rate together with a very long gain lifetime.[10] This concurs with results obtained for spherical CdSe core−giant CdS shell nanocrystals.[11−15] Despite these numerous observations, open questions remain regarding the actual band alignment and its influence on the radiative recombination processes. Optical measurements proposed a quasi-type-II alignment in which the electron wave function is fully delocalized over the rod while the hole wave function is localized in the core region (Figure 1b).[8,16,17] In addition, *ab initio*

* Address correspondence to gra@zurich.ibm.com, zeger.hens@ugent.be, rfm@zurich.ibm.com.

Received for review February 14, 2011 and accepted April 13, 2011.

Published online April 19, 2011
10.1021/nn2005969

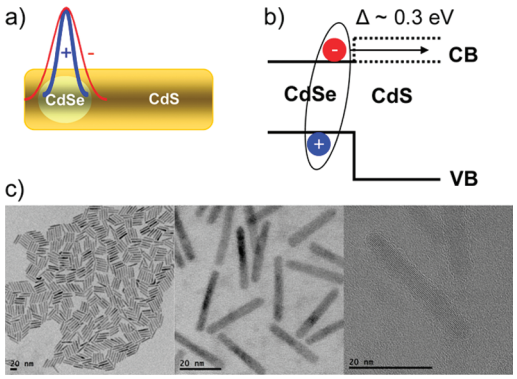

Figure 1. (a) Sketch of the dot-in-rod structure and of the electron and hole spatial wave function distributions. (b) Illustration of the band alignment for two conduction band offsets ($\Delta \sim 0$ and $\Delta \sim 0.3$ eV). (c) Representative TEM images of CdSe/CdS nanorods, core size 3.3 nm, rod length 29.3 $\pm$ 2.4 nm, and rod width 4.1 $\pm$ 0.4 nm.

quality charge patching method calculations resulted in a complete type-II configuration.[18] In contrast, scanning tunneling spectroscopy (STS) studies[19] and optical measurements,[20,21] reinforced by envelope-function theoretical calculations, suggested a conduction band offset of $\Delta \sim 0.3$ eV with the possibility to change from type-I to a quasi-type-II regime by tuning the core diameter.

As the understanding and control of the band alignment are prerequisite to harness the unique opto-electronic properties of these dot-in-rod structures, further experimental work clarifying the (de)localization of the electron wave function is mandatory.

Here, we investigate CdSe/CdS dot-in-rod structures that exhibit almost no thermally induced quenching of the photoluminescence, which is indicative of a negligible density of defect states at the CdSe/CdS interface and the CdS surface. This allows us to study the electron (de)localization by means of time-resolved photoluminescence (PL) measurements. Indeed, we observe a clear size-dependent radiative lifetime, which can be linked to the different degree of localization of the electron wave function. Moreover, the exciton radiative lifetime is found to increase with increasing temperature, an uncommon feature that has not been reported so far for such a material system. In principle, this behavior can be explained by considering the occurrence of different processes: (i) an exciton redistribution in momentum space along with phonon/defect scattering,[22] (ii) a detrapping process from trap states to the exciton states,[23] (iii) the contribution of a thermally populated higher emitting state with a different oscillator strength, (iv) a temperature-dependent band offset with a consequently different degree of localization for the electron wave function. In the present work, we provide a thorough study on a set of samples that supports the last hypothesis.

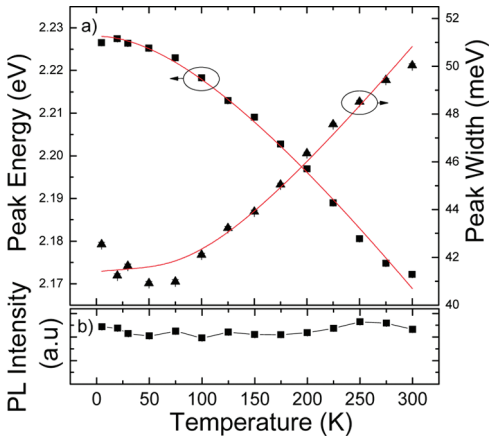

Figure 2. (a) Temperature dependence of the PL emission peak energy (solid squares) and width (solid triangles). The solid lines are fits using the Varshni law and the exciton–phonon model for the temperature variation of the energy and width, respectively. (b) Integrated PL intensity *vs* temperature. No appreciable PL quenching is observed.

RESULTS AND DISCUSSION

CdSe/CdS nanorods were synthesized according to an established procedure,[6] allowing a narrow size distribution of nanorod diameters and lengths. Figure 1c shows a typical transmission electron microscopy (TEM) image, illustrating the narrow dispersion in rod diameters and lengths of the samples used (see Figure S1 in the Supporting Information for statistical analysis of the lengths and diameters of all samples used in this study).

First, we investigated the change of the PL spectrum as a function of temperature T. Figure 2 reports the results obtained by fitting a single Gaussian function to the PL spectrum recorded at different temperatures (the raw spectra are shown in Figure S2 in the Supporting Information). As expected, the PL peak energy shifts toward lower energy owing to the lattice deformation potential and exciton–phonon coupling, which leads to a smaller energy band gap. The experimental data are well-fitted by the empirical Varshni law for the band gap $E_g(T) = E_g(T = 0) - \alpha T^2/(T + \beta)$, as reported in Figure 2a. The resulting fitting parameters ($\alpha \sim 5 \times 10^{-4}$ eV/K; $\beta \sim 250$ K) are, in first approximation, similar to those of bulk CdSe material.[24,25] This suggests that the emission originates mainly from electrons and holes near the band edge of the CdSe core. The temperature dependence of the PL peak width has been fitted using the exciton–phonon model, which has been successfully applied to similar heterostructures before.[24,25] Here, the peak width is given by $\Gamma(T) = \Gamma_{inh} + \Gamma_{AC}\,T + \Gamma_{LO}(\exp(-E_{LO}/(kT)) - 1)$, where Γ_{inh} is the inhomogeneous width, Γ_{AC} the exciton–acoustic phonon coupling coefficient, Γ_{LO} the exciton–LO phonon coupling coefficient, E_{LO} the LO phonon energy, and k the Boltzmann constant. Again, the parameters extracted ($\Gamma_{inh} \sim 40$ meV, $\Gamma_{AC} \sim 5\ \mu$eV/K, $\Gamma_{LO} \sim 18$ meV, $E_{LO} \sim 30$ meV) are similar to the

values reported in literature.[24,25] Finally, Figure 2b reports the PL intensity as function of temperature. No appreciable drop in the PL intensity has been observed, pointing toward a strong suppression of the thermally activated nonradiative recombination processes. This is probably due to the reduced density of defect states at the interface, which are commonly thought to be efficient trap centers giving rise to nonradiative decay.[24−26] In contrast, the PL intensity of typical CdSe/ZnS QDs decreases with increasing temperature, as often reported in literature (see Figure S3 in the Supporting Information).[24−26] Indeed, the use of a CdS shell with a lower lattice mismatch (than the ZnS) minimizes the occurrence of defects and/or dislocations, which otherwise strongly quench the PL intensity. It is worth noting that the resulting electronic configuration in such heterostructures (*i.e.*, the number of states localized in the core region and their energy separation) could also play an important role in the suppression of the temperature-induced quenching process.[24,25]

To gain more insight into the underlying decay process, we performed time-resolved PL experiments as a function of temperature, as reported in Figure 3. The traces can be fitted by a monoexponential decay function up to room temperature with a typical decay time of some tens of nanoseconds. An increase of the exciton lifetime with temperature is clearly observed. This confirms the hypothesis that a single effective state contributes to the radiative recombination. In contrast, in CdSe/ZnS QDs, the lifetime decreases with temperature and becomes strongly nonexponential (see Figure S4 in the Supporting Information). The observed increase of the exciton lifetime in the dot-in-rod structures can be explained by considering the different effects already outlined above. In order to narrow down on the relevant processes, we extended our investigation to a set of samples having different core diameters, ranging from 2.2 to 3.3 nm, while maintaining the same shell shape and thickness (the statistical TEM analysis can be found in the Supporting Information).

Figure 4 summarizes the experimental results. In Figure 4a, the energy difference between the exciton absorption peaks of core-only and core−shell structures is plotted as a function of the core diameter (see Figure S2 in the Supporting Information for the full absorption spectra). A larger red shift is observed for structures having smaller cores. In addition, the room-temperature exciton lifetimes are plotted *versus* the core diameter. It is evident that smaller core heterostructures exhibit a longer exciton lifetime (see also the inset of Figure 4a). If the CdSe/CdS dot-in-rods behaved as simple CdSe core QDs, the opposite trend would be observed, that is, a decreasing radiative lifetime with decreasing core size.[27] Therefore, we interpret these observations in terms of a changing delocalization of the electron wave function in the shallow potential well that is formed by the CdSe/CdS heterostructure. In other words, the smaller cores

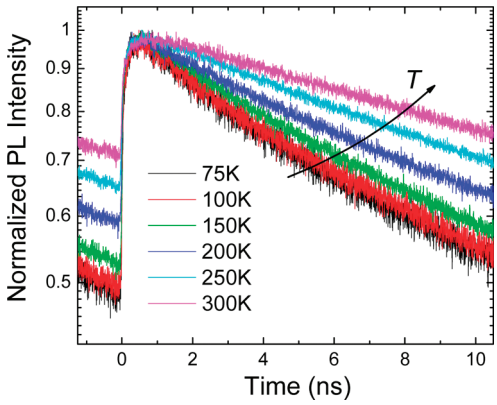

Figure 3. Time-resolved PL measurements *vs* temperature. A clear increase in the exciton lifetime is observed.

exhibit larger electron delocalization, and consequently, they show a longer radiative lifetime. The hole levels are affected less and remain confined in the core region because of the higher valence band offset and the higher hole effective mass.[20] It is worth noting that, since the shape of the rod remains almost the same by changing the core size, the change in shell thickness may also contribute to the observed increase in the electron delocalization for smaller core heterostructures.

Figure 4b shows the measured exciton lifetimes as a function of temperature for all samples studied. Between 75 and 300 K, we systematically find a size-dependent radiative lifetime. In particular, at 75 K, the lifetime changes from 16 to 8 ns for 2.2 and 3.3 nm core-size samples, respectively. This drop by a factor of 2 agrees well with the computed electron−hole overlap based on the envelope function approximation and an offset of $\Delta \sim$ 0.3 eV between the CdSe and the CdS conduction band.[20]

Moreover, in all samples studied, an increase in the exciton lifetime with temperature is observed. This behavior cannot be related to the influence of defect states (hypothesis (ii)) or to a higher energy state with different oscillator strength (hypothesis (iii)). Indeed, one would expect the PL to be quenched at higher temperature because of the trapping process and a non-exponential decay in the latter case. On the other hand, it is well-known that an increase in temperature (or pressure and strain[28−30]) alters the conduction and valence band energies in semiconductors and semiconductor nanocrystals. This is mainly due to the interaction with the lattice vibrations and a volume change. Consequently, the band offset is also temperature-dependent because the energy bands in each semiconductor forming the heterojunction will exhibit a temperature dependence related to the semiconductor's own crystal structure (see Figure S6 in the Supporting Information). Moreover, temperature can alter the amount of accumulated charges at the interface with a net change in the built-in potential. In this way, the experimentally observed prolonging of the radiative exciton lifetime points toward an increased electron

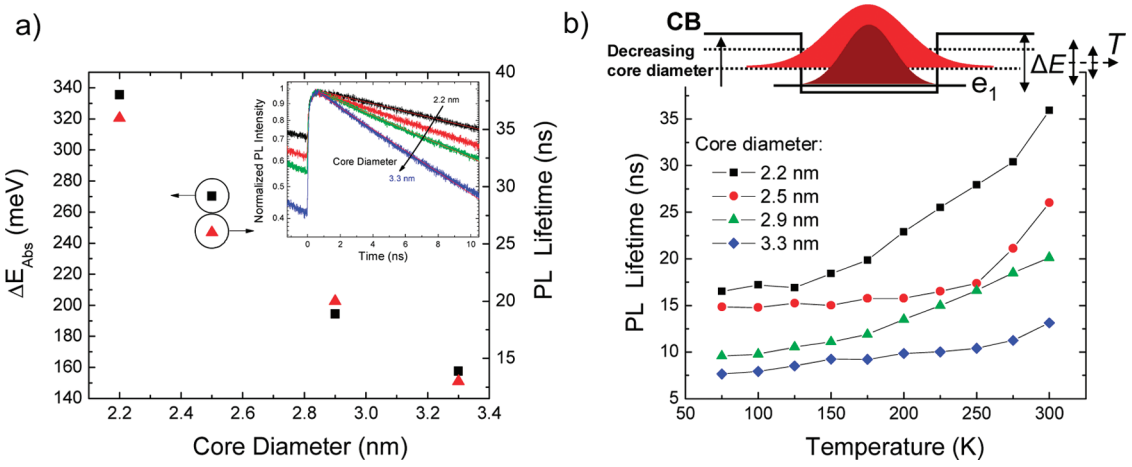

Figure 4. (a) Energy difference ΔE_{Abs} (black squares) between the first exciton absorption peak in core-only and core/shell structures together with the PL lifetime (red triangles) as a function of the core diameter, measured at room temperature. The inset shows the time-resolved PL traces for the four different samples. (b) Temperature dependence of the PL lifetime for all core diameters studied. The sketch illustrates the expected conduction band configuration, i.e., the change in the energy levels for different core diameters; the different degree of wave function delocalization together with the decrease of the conduction band offset (ΔE) as a function of the temperature T.

TABLE 1. Sizes of the CdSe/CdS Nanorods Used

CdSe core size (nm)	length (nm)	diameter (nm)
2.2	37.6 ± 2.3	4.7 ± 0.5
2.5	27.3 ± 3.3	4.8 ± 0.5
2.9	29.9 ± 2.3	4.5 ± 0.5
3.3	29.3 ± 2.4	4.1 ± 0.4

delocalization resulting from a reduction of the conduction band offset with increasing temperature. It is worth pointing out that the increase in the lifetime starts to be effective at relatively high temperatures (>100 K, see Figure 3), which is the temperature range where the energy gap starts to shift strongly toward lower energy (Figure 2). This provides additional support for hypothesis (iv) that the increasing radiative lifetime is mainly due to a change of the band-offset (ruling out hypothesis (i), which occurs at very low temperature). However, as the change of the core diameter involves other intricate changes (*i.e.*, electronic states, volume, coupling to the phonons[31]), there is no simple relation that can quantitatively describe the slightly different temperature dependencies of the different samples.

CONCLUSION

In summary, we reported on the radiative recombination process occurring in high-quality CdSe/CdS dot-in-rod structures. We observed that the thermally induced PL quenching is almost absent, which enables us to access the radiative decay directly without non-radiative processes concealing the effects of the wave function delocalization. A clear increase of the radiative lifetime with decreasing CdSe dot size has been observed, caused by the different degree of localization of the electronic wave function. Quantitatively, the change in lifetime agrees well with a conduction band offset of 0.3 eV, as proposed earlier in the literature.[19,20] Moreover, the exciton lifetime increases with temperature owing to a change in the band offset. These results indicate that the degree of electron localization in the lowest conduction band level can be controlled by the size of the core and the temperature. This also suggests that results obtained at low temperature should be used with care when explaining experiments conducted at room temperature.

A comprehensive quantum description of the electron−phonon coupling,[31] the band-offset, and the electron−hole exchange interaction would be required to explain quantitatively the temperature dependence of different core sizes. Understanding and controlling the electron (de)localization in these colloidal dot-in-rod nanocrystals will provide the grounds for realizing efficient and low-cost light-emitting devices.

EXPERIMENTAL SECTION

Sample Preparation. CdSe/CdS nanorods were synthesized according to a published procedure.[6] First, CdSe cores (seeds) are synthesized in trioctylphosphinoxide (TOPO), using a mixture of cadmium oxide (CdO) octadecylphosphonic acid and trioctylphosphineselenide (TOPSe) as precursors. The CdSe cores have a band gap in the range 480−600 nm. The QD size d is determined according to the sizing curve of Jasieniak *et al.*[32] The QD concentration in suspension C is calculated from Beer's law ($A = \varepsilon CL$, where L is the sample length). We use the absorbance at 350 nm A_{350} and a molar extinction coefficient ε_{350} obtained from the size-independent absorption coefficient at 350 nm:[32]

$$\varepsilon_{350} = 0.01685 \times d^3 \text{ cm}^{-1}/\mu\text{M}$$

To synthesize the CdSe/CdS nanorods, the CdSe seeds are co-injected with a TOPS precursor into a hot reaction mixture that contains octadecyl- and hexylphosphonic acid, TOPO and CdO.

Structural Characterization. Transmission electron microscopy (TEM) measurements were carried out using a JEOL FE2200. Analysis of the nanorod length and diameter was performed using DigitalMicrograph software. Table 1 summarizes the dimensions of the nanorods used throughout this work.

Optical Characterization. For optical measurements, a thin film was prepared by drop-casting the QD solutions on a precleaned glass substrate. Luminescence spectroscopy was performed by exciting the samples with a frequency-doubled Ti:sapphire mode-locked laser delivering pulses of about 150 fs duration at 400 nm and a repetition rate of 80 MHz. Time-integrated photoluminescence was analyzed using a CCD-coupled grating spectrometer. Time-resolved photoluminescence was recorded by an avalanche photodiode (APD) in combination with a time-correlated single-photon counting (TCSPC) module. The experimental time resolution is about 100 ps.

Acknowledgment. We thank B. Mazenauer and D. Caimi for their technical support, and B.J. Offrein for stimulating discussions. The research leading to these results has received funding from the European Community's Seventh Framework Programme under Grant Agreement No. 214954 (HERODOT). I.M. is a postdoctoral researcher with the FWO-Vlaanderen.

Supporting Information Available: We provide additional information on the structural (statistics on particles size distribution) and optical properties of CdSe/CdS dot-in-rod structures. Typical results of CdSe/ZnS QDs are also reported for comparison. This material is available free of charge *via* the Internet at http://pubs.acs.org.

REFERENCES AND NOTES

1. Coe, S.; Woo, W. K.; Bawendi, M. G.; Bulovic, V. Electroluminescence from Single Monolayers of Nanocrystals in Molecular Organic Devices. *Nature* **2002,** *420*, 800.
2. Greenham, N. C.; Peng, X.; Alivisatos, A. P. Charge Separation and Transport in Conjugated-Polymer/Semiconductor-Nanocrystal Composites Studied by Photoluminescence Quenching and Photoconductivity. *Phys. Rev. B* **1996,** *54*, 17628.
3. Klimov, V. I.; Mikhailovsky, A. A.; Xu, S.; Malko, A.; Hollingworth, J. A.; Leatherdale, C. A.; Eisler, H.-J.; Bawendi, M. G. Optical Gain and Stimulated Emission in Nanocrystal Quantum Dots. *Science* **2000,** *290*, 314.
4. Hewa-Kasakarage, N. N.; Kirsanova, M.; Nemchinov, A.; Schmall, N.; El-Khoury, P. Z.; Tarnovsky, A. N.; Zamkov, M. Radiative Recombination of Spatially Extended Excitons in (ZnSe/CdS)/CdS Heterostructured Nanorods. *J. Am. Chem. Soc.* **2009,** *131*, 1328–1334.
5. Talapin, D. V.; Koeppe, R.; Götzinger, S.; Kornowski, A.; Lupton, J. M.; Rogaci, A. L.; Benson, O.; Feldmann, J.; Weller, H. Highly Emissive Colloidal CdSe/CdS Heterostrucutres of Mixed Dimensionality. *Nano Lett.* **2003,** *3*, 1677–1681.
6. Carbone, L.; Nobile, C.; De Giorgi, M.; Della Sala, F.; Morello, G.; Pompa, P.; Hytch, M.; Snoeck, E.; Fiore, A.; Franchini, I. R.; *et al.* Synthesis and Micrometer-Scale Assembly of Colloidal CdSe/CdS Nanorods Prepared by a Seeded Growth Approach. *Nano Lett.* **2007,** *7*, 2942–2950.
7. Talapin, D. V.; Nelson, J. H.; Shevchenko, E. V.; Aloni, S.; Sadtler, B.; Alivisatos, A. P. Seeded Growth of Highly Luminescent CdSe/CdS Nanoheterostructures with Rod and Tetrapod Morphologies. *Nano Lett.* **2007,** *7*, 2951–2959.
8. Müller, J.; Lupton, J. M.; Lagoudakis, P. G.; Schindler, F.; Koeppe, R.; Rogach, A. L.; Feldmann, J.; Talapin, D. V.; Weller, H. Wave Function Engineering in Elongated Semiconductor Nanocrystals with Heterogeneous Carrier Confinement. *Nano Lett.* **2005,** *5*, 2044–2049.
9. Pisanello, F.; Martiradonna, L.; Leménager, G.; Spinicelli, P.; Fiore, A.; Manna, L.; Hermier, J. P.; Cingolani, R.; Giacobino, E.; De Vittorio, M.; Bramati, A. Room Temperature Dipole-like Single Photon Source with a Colloidal Dot-in-Rod. *Appl. Phys. Lett.* **2010,** *96*, 033101.
10. Zavelani-Rossi, M.; Lupo, M. G.; Tassone, F.; Manna, L.; Lanzani, G. Suppression of Biexciton Auger Recombination in CdSe/CdS Dot/Rod: Role of the Electronic Structure in the Carrier Dynamics. *Nano Lett.* **2010,** *10*, 3142–3150.
11. Mahler, B.; Spinicelli, P.; Buil, S.; Quelin, X.; Hermier, J.-P.; Dubertret, B. Towards Non-blinking Colloidal Quantum Dots. *Nat. Mater.* **2008,** *7*, 659–664.
12. García-Santamaría, F.; Chen, Y.; Vela, J.; Schaller, R. D.; Hollingsworth, J. A.; Klimov, V. I. Suppressed Auger Recombination in "Giant" Nanocrystals Boosts Optical Gain Performance. *Nano Lett.* **2009,** *9*, 3482–3488.
13. Chen, Y.; Vela, J.; Htoon, H.; Casson, J. L.; Werder, D. J.; Bussian, D. A.; Klimov, V. I.; Hollingsworth, J. A. "Giant" Multishell CdSe Nanocrystal Quantum Dot with Suppressed Blinking. *J. Am. Chem. Soc.* **2008,** *130*, 5026–5027.
14. Htoon, H.; Malko, A. V.; Bussian, D.; Vela, J.; Chen, Y.; Hollingsworth, J. A.; Klimov, V. I. Highly Emissive Multiexcitons in Steady-State Photoluminescence of Individual "Giant" CdSe/CdS Core/Shell Nanocrystals. *Nano Lett.* **2010,** *10*, 2401–2407.
15. Jha, P. P.; Guyot-Sionnest, P. Trion Decay in Colloidal Quantum Dots. *ACS Nano* **2009,** *3*, 1011–1015.
16. Muller, J.; Lupton, J. M.; Rodach, A. L.; Feldmann, J.; Talapin, D. V.; Weller, H. Monitoring Surface Charge Movement in Single Elongated Semiconductor Nanocrystals. *Phys. Rev. Lett.* **2004,** *93*, 167402.
17. Lupo, M. G.; Della Sala, F.; Carbone, L.; Zavelani-Rossi, M.; Fiore, A.; Lüer, L.; Polli, D.; Cingolani, R.; Manna, L.; Lanzani, G. Ultrafast Electron-Hole Dynamics in Core/Shell CdSe/CdS Dot/Rod Nanocrystals. *Nano Lett.* **2008,** *8*, 4582–4587.
18. Luo, Y.; Wang, L.-W. Electronic Structures of the CdSe/CdS Core−Shell Nanorods. *ACS Nano* **2010,** *4*, 91–98.
19. Steiner, D.; Dorfs, D.; Banin, U.; Della Sala, F.; Manna, L.; Millo, O. Determination of Band Offsets in Heterostructured Colloidal Nanorods Using Scanning Tunneling Spectroscopy. *Nano Lett.* **2008,** *8*, 2954–2958.
20. Sitt, A.; Della Sala, F.; Menagen, G.; Banin, U. Multiexciton Engineering in Seeded Core/Shell Nanorods: Transfer from Type-I to Quasi-Type-II Regimes. *Nano Lett.* **2009,** *9*, 3470–3476.
21. Morello, G.; Della Sala, F.; Carbone, L.; Manna, L.; Maruccio, G.; Cingolani, R.; De Giorgi, M. Intrinsic Optical Nonlinearity in Colloidal Seeded Grown CdSe/CdS Nanostructures: Photoinduced Screening of the Internal Electric Field. *Phys. Rev. B* **2008,** *78*, 195313.
22. Zhang, X. H.; Chua, S. J.; Yong, A. M.; Yang, H. Y.; Lau, S. P.; Yu, S. F.; Sun, X. W.; Miao, L.; Tanemura, M.; Tanemura, S. Exciton Radiative Lifetime in ZnO Nanorods Fabricated by Vapor Phase Transport Method. *Appl. Phys. Lett.* **2007,** *90*, 013107.
23. Jones, M.; Lo, S. S.; Scholes, G. D. Signatures of Exciton Dynamics and Carrier Trapping in the Time-Resolved Photoluminescence of Colloidal CdSe Nanocrystals. *J. Phys. Chem. C* **2009,** *113*, 18632–18642.
24. Valerini, D.; Creti, A.; Lomascolo, M.; Manna, L.; Cingolani, R.; Anni, M. Temperature Dependence of the Photoluminescence Properties of Colloidal CdSe/ZnS Core/Shell Quantum Dots Embedded in a Polystyrene Matrix. *Phys. Rev. B* **2005,** *71*, 235409.
25. Jing, P.; Zheng, J.; Ikezawa, M.; Liu, X.; Lv, S.; Kong, X.; Zhao, J.; Masumoto, Y. Temperature-Dependent Photoluminescence of CdSe-Core CdS/CdZnS/ZnS-Multishell Quantum Dots. *J. Phys. Chem. C* **2009,** *113*, 13545–13550.
26. Sarma, D. D.; Nag, A.; Santra, P. K.; Kumar, A.; Sapra, S.; Mahadevan, P. Origin of the Enhanced Photoluminescence from Semiconductor CdSeS Nanocrystals. *J. Phys. Chem. Lett.* **2010,** *1*, 2149–2153.
27. van Driel, A. F.; Allan, G.; Delerue, C.; Lodahl, P.; Vos, W. L.; Vanmaekelbergh, D. Frequency-Dependent Spontaneous

Emission Rate from CdSe and CdTe Nanocrystals: Influence of Dark States. *Phys. Rev. Lett.* **2005,** *95*, 236804.
28. Choi, C. L.; Koski, K. J.; Sivasankar, S.; Alivisatos, A. P. Strain-Dependent Photoluminescence Behavior of CdSe/CdS Nanocrystals with Spherical, Linear, and Branched Topologies. *Nano Lett.* **2009,** *9*, 3544–3549.
29. Smith, A. M.; Mohs, A. M.; Nie, S. Tuning the Optical and Electronic Properties of Colloidal Nanocrystals by Lattice Strain. *Nat. Nanotechnol.* **2009,** *4*, 56–63.
30. Yang, S.; Prendergast, D.; Neaton, J. B. Strain-Induced Band Gap Modification in Coherent Core/Shell Nanostructures. *Nano Lett.* **2010,** *10*, 3156–3162.
31. Kelley, A. M. Electron−Phonon Coupling in CdSe Nanocrystals. *J. Phys. Chem. Lett.* **2010,** *1*, 1296–1300.
32. Jasieniak, J.; Smith, L.; van Embden, J.; Mulvaney, P.; Califano, M. Re-examination of the Size-Dependent Absorption Properties of CdSe Quantum Dots. *J. Phys. Chem. C* **2009,** *113*, 19468–19474.